2.2 Lattice

Editorial note: Oct. 98 handbook update suffered lack of time and is thus incomplete. Sections 2.2.0-2.2.5 follow Jan. 98 version with some minor updates concerning the new (but yet incompletely elaborated) lattice mode D2A and the new design energy of 2.4 GeV (before: 2.1 GeV). Section 2.2.6 on closed orbit correction and coupling control is new. Vertical vacuum chamber has been reduced from 35 to 32 mm full height. This minor change slightly affects some data and figures and was not included in section 2.2.0-2.2.5 update.

2.2.0 Definitions

- The *ideal lattice* as the first level of design is the magnet configuration of one period of the storage ring. No particular beam energy is assumed, energy dependent parameters like e.g. emittance are simply calculated by scaling.

  The ideal lattice is used for design and exploration of linear and non-linear beam dynamics in the framework of Hamiltonian theory. Studies of off-momentum optics in the ideal lattice ignore synchrotron oscillations and treat the relative momentum deviation $\delta =: \Delta p/p$ as a parameter of the lattice (adiabatic approximation).

- The *bare lattice* as the second level of design is the full storage ring lattice at a particular beam energy, including RF cavities, with all elements error free.

- The *real lattice* as the third level of design eventually includes errors like alignment errors, higher order multipoles etc.

- *Effective emittance* is the apparent emittance of a beam widened by momentum spread σ_δ in a dispersive region ($\eta \neq 0$) and at a symmetry point of the lattice given by

$$\varepsilon_{eff} = \varepsilon_0 \sqrt{1 + \frac{(\sigma_\delta \eta)^2}{\varepsilon_0 \beta_x}}$$

- *Dynamic horizontal (vertical) acceptance* is the phase space area enclosed by a particle starting at a horizontal (vertical) amplitude, that is at the boundary of short term stability, and with the vertical (horizontal) amplitude very small but nonzero. Clearly the acceptance will depend on the number of turns tracked.

- *Dynamic aperture* is the local projection of the acceptance from phase space to physical space.

- *Momentum acceptance* as defined from the Touschek scattering point of view is the interval of relative momentum deviation $\delta =: \Delta p/p$ where a Touschek scattered particle from the beam core, i.e. x, p_x, y, p_y small and momentum deviation suddenly changed to δ, remains inside the momentum dependent transverse acceptance. Thus momentum acceptance depends on the lattice functions at the location where the scattering occurred. We define the Touschek relevant effective lattice momentum acceptance (TRELMA) as the value of RF acceptance where a calculation with only the RF acceptance (assuming infite lattice acceptances) and a calculation with only the lattice acceptance (assuming infinite RF acceptance) give the same result for the Touschek lifetime (normalised to bunch length) [7]. We further distinguish between the physical TRELMA, defined by the physical acceptance alone (assuming an ideally linear lattice) and the dynamic TRELMA, defined by the dynamic acceptance (assuming an infinetely wide beampipe).

2.2.1 Design goals and how they are fulfilled

Energy 2.4 GeV.

The lattice is designed for 2.4 GeV ($B\rho$ = 8 Tm).

Circumference less than 300 m with convenient prime factor decomposition of the harmonic number in order to allow many different bunch patterns.

Circumference = 288 m. Harmonic number = 480 = $2^5 \cdot 3 \cdot 5$ with 500 MHz RF-systems.

Emittance < 5 nm at 2.4 GeV

Emittance = 4.8 nm at 2.4 GeV with dispersion free straight sections. With dispersion in the straight sections the effective emittance is about 4.1 nm.

At least eight straight sections with at least each two of length ≥11 m, 7 m and 4 m.

3×11.76 m, 3×7.00 m, 6×4.00 m.

Large transverse acceptances for safe operation

Ideal lattice dynamic acceptances of approx. 80 μm·rad horizontal and 50 μm·rad vertical exceed the physical acceptances (45 resp. 13 μm·rad).

Large momentum acceptance for long Touschek lifetime

A TRELMA of 5.4 % provides 23 hours of Touschek lifetime for a 1 nCb/bunch (or 1.04 mA/bunch) beam at 2.4 GeV with 1% emittance coupling and 2.6 MV RF voltage (see [7] and section 2.7).

Low emittance coupling for highest brightness

A coupling factor down to 0.25 % was achieved in simulations after careful closed orbit correction with realistic misalignment errors.

Simplicity, i.e. large periodicity and symmetry, few magnet types.

Periodicity 3, symmetry 3.

2 bending magnet types, 3 quadrupole types, 1 sextupole type, correctors included as additional windings in sextupoles.

Mini-beta-straights for mini gap undulators and wavelenght shifters.

Triplets or quadruplets on each side of the straights for optimal matching to the insertion devices.

Possibility to install later superconducting bending magnets

The centre bends of the proposed TBA structure could well be replaced by superconducting bends.

Flexibility.

Several operation modes are feasible:

- standard mode (D0): zero dispersion in straights, mini-beta-straights, 4.8 nm emittance
- low emittance (D1): nonzero dispersion, 3.9 nm emittance (4.1 nm effective)
- new standard mode (D2A): like D0 but with another working point providing lower emittance coupling on some expense of dynamic aperture
- relaxed: large beta functions in the straights and large emittance, for commissioning
- isochronous: zero momentum compaction

2.2.2 Lattice concept and design outline

Choice of TBA (triple bend achromat)

Dedicated synchrotron light source lattices consist of achromatic arcs and dispersion free straight sections. The bending angle φ of the arc dipoles has to be sufficiently small to obtain the desired low emittance due to $\varepsilon \propto \varphi^3$. In case of SLS $\varphi \approx 10°$.

N bending magnets form an NBA (N bend achromat) arc. Extensive previous work focusing on $N \geq 4$ lattices, in particular on a 7BA hexagon [1,2] lead to the conclusion, that those lattices are restricted in flexibility concerning the variation of operation modes and the possibilities of non-linear optics optimisation for obtaining sufficient dynamic acceptances. On the other hand a DBA lattice ($N = 2$) of desired emittance would end up at too large circumference. A TBA lattice ($N = 3$) was found to be the best and only choice to fulfil all design goals.

Number of TBA cells

Low emittance demands a small angle per bending magnet, i.e. a large number of TBAs. On the other hand the limitation on the circumference of 300 m limits their number. A compromise is found for an angle per bending magnet of about 10°.

A lattice made from 12 TBAs was found to accommodate the three different types of straights well in a structure of reasonably large periodicity (3) and 3-fold mirror symmetry. Alternative TBA lattices like a period-2 lattice made from 14 TBAs or an asymmetric period-4 12 TBA lattice were tested and found to be inferior in performance, i.e. in flexibility and dynamic acceptances.

TBA design

A TBA consists of two end bending magnets which create and suppress the dispersion and a centre bending magnet with a beam waist at its middle. The minimum emittance achievable for an end bend, where $\eta = 0$ on one side is by a factor 3 larger than for a centre bend, where $\eta' = 0$ in the middle [3].

The distribution of bending angles on the centre bend and the end bends had to be optimised considering emittance and dynamic acceptances:

Emittance grows with the cube of the bending angle and is an additive quantity ($\varepsilon \propto \langle H \rangle_{mag}$). If we assume that the beam parameters for all bends fulfil to same extent, expressed by a factor F, the condition to achieve the theoretical minimum emittance, we get $\varepsilon = 52\ \text{nm}\cdot\text{rad}\cdot F\cdot(\varphi_c^3 + 2\cdot b\cdot\varphi_e^3)$ (for E = 2.1 GeV and $J_x = 1$), with φ_c and φ_e the angles of the centre and the end bend; b = 3 for a lattice with dispersionfree straights (D0) and b = 1 for distributed dispersion (D1). With the total TBA deflection angle $\Phi = \varphi_c + 2\cdot\varphi_e$ fixed we find for the minimum emittance $\varphi_c = (\sqrt{12} - 3)\cdot\Phi$ for D0-mode and, as expected, $\varphi_c = \Phi/3$ for D1-mode. With $\Phi = 30°$ this gives $\varphi_c = 13.9°$ (D0) and $\varphi_c = 10°$ (D1). The corresponding emittances are 3.2 nm·rad (D0) and 1.9 nm·rad (D1) for F = 2.

Further optimisation emphasized dynamic acceptance. Design goal was to achieve dynamic acceptances of the ideal lattice exceeding the physical ones for the ideal lattice in order to remain with dynamic acceptances at least comparable to the physical ones for the real lattice, and with it gurarantee operational safety and sufficient lifetime.

For a lattice in D1-mode excellent solutions were obtained with 10°–10°–10° TBAs with dispersion ranging between 12 and 20 cm in the straight sections. Unfortunately a reasonable D0-mode was found inaccessible for that lattice. For a lattice in D0-mode good solutions had to stay close to the half bend dispersion suppressor scheme of a 7½°–15°–7½° TBA.

Since D0 and D1-mode were found incompatible, priority was set in favour of the D0-mode, mainly due to the fact, that momentum jitter, widening, etc. should not be visible on the photon beam. Eventually a 8°–14°–8° TBA was chosen to provide minimum emittances in D0-mode at sufficient dynamic acceptance. The D1 mode of this lattice is similar to the D0-mode and has very small dispersion in the straights.

Limitation of magnet strengths

Based on a comparison of ten existing or proposed storage rings we assume for the maximum poletip fields:

- 1.40 T in bending magnets (bending radius $|\rho_0| = 5.71$ m)
- 0.65 T in quadrupoles
- 0.37 T in sextupoles

At 2.4 GeV the magnetic rigidity is $(B\rho) = 8$ Tm. From that follow the maximum magnet strengths:

- The aperture radius for quadrupoles, i.e. the radius of the pole inscribed circle, is $R = 30$ mm, see section 2.3 or [4]. This gives for the limitation of gradient and strength: $|B'| \leq 21.7$ T/m and $|b_2| \leq 2.7$ m^{-2}.
- The aperture radius for sextupoles is $R = 34$ mm, see section 2.3. This gives for the 2nd derivative of the field and for the sextupole strength
  $\left|B'' =: \frac{B_{poletip}}{R^2/2}\right| \leq 640$ T/m^2 and $\left|b_3 =: \frac{B''}{2(B\rho)}\right| \leq 40$ m^{-3}.

Distances

The minimum distances between magnets along the ring are limited by the demands from the vacuum system (see section 2.6). Following values were assumed during the optics design:

- 0.40 m between bending magnet and quadrupole in order to accommodate a flange and an absorber or a flange and a bellow.
- 0.26 m between quadrupole and sextupole if there is an absorber.
- 0.16 m between quadrupole and sextupole if there is a beam position monitor or nothing.

The length of the straight sections are

- 11.76 m (DL) for the three long straights,
- 7.00 m (DM) for the three medium straights,
- 4.00 m (DS) for the six short straights.

All these distances refer to the magnetic lengths of the elements.

Magnet types and families

The magnetic lengths were chosen to cover all probable operation modes of the lattice without exceeding the maximum strength values. The table below summarises the magnet types:

Type	Number	Length	Fields and strengths at 2.4 GeV
Bending magnets	12 24	1.40 m 0.80 m	$B = 1.40$ T, $B' = 0$
Quadrupoles	54 54 66	0.20 m 0.32 m 0.44 m	$\lvert B_{PT} \rvert \leq 0.65$ T, $\lvert B' \rvert \leq 21.7$ T/m, $\lvert b_2 \rvert \leq 2.7$ m^{-2}
Sextupoles	120	0.20 m	$\lvert B_{PT} \rvert \leq 0.37$ T, $\lvert \int b_3 dl \rvert \leq 8$ m^{-2}

Figure f22_a shows the layout of one of the 12 TBA structures including the sections for matching to the straights. Four quadrupoles are required for matching to the long straight, each three for matching to the medium and short straights. Also the quadrupoles inside the TBA contribute to the matching.

The numbers of magnet families:

- The 36 bending magnets (2 types) will all be connected in series, thus forming one family.
- The 174 quadrupoles (3 types) will be individually powered to allow highest flexibility, i.e. every quadrupole is its own family. 22 families would be the minimum, with 7, resp. 8 families for matching from the TBA centres to the three types of straight sections.
- The 120 sextupoles (1 type) are grouped into 9 families, 3 of them mainly chromatic and 6 geometric. This configuration was found to be adequate in most cases to suppress the nine first order sextupole modes and beyond it to minimise the second order modes in order to optimise the dynamic acceptances (see below).

2.2.3 Lattice performance optimisation strategy

Historically the approach to optimisation of lattice performance proceeded in two consecutive steps by designing the linear optics first and adding the non-linear optimisation later by tuning „harmonic sextupoles“. This was successfully applied to many machines. However, modern high performance light sources like SLS are strongly non-linear machines since pushing for low emittance needs strong quadrupoles, which, in turn, require strong sextupoles for compensation of the large linear chromaticities. This type of lattice for producing high brightness synchrotron light requires a procedure of interleaved linear *and* non-linear optimisation. Since the need to suppress non-linear perturbations puts serious constraints on general lattice layout and linear optics design, as it turned out during the long process of lattice optimisation, we have now the somewhat unusual situation, that the description of the optics has to start with non-linear dynamics.

First order optimisation

The nine driving terms in first order of sextupole strength b_3 of the one-turn map are four chromatic and five geometric modes. They are given by [2]

$$h_{jklmp} \propto \sum_{n}^{N_{sext}} (b_3 l)_n \beta_{xn}^{\frac{j+k}{2}} \beta_{yn}^{\frac{l+m}{2}} \eta_n^p e^{i\{(j-k)\mu_{xn}+(l-m)\mu_{yn}\}} \underbrace{- \sum_{n}^{N_{quad}} (b_2 l)_n \beta_{xn}^{\frac{j+k}{2}} \beta_{yn}^{\frac{l+m}{2}} e^{i\{(j-k)\mu_{xn}+(l-m)\mu_{yn}\}}}_{if \quad p \neq 0}$$

with j, k, l, m, p integers. ($b_2 l$) and ($b_3 l$) are the integrated quadrupole and sextupole strengths. β, η, μ are the beta functions, dispersion and betatron phases. Every sextupole, and for the chromatic modes ($p \neq 0$) every quadrupole too, is represented by a complex vector.

h_{11001} and h_{00111} are effectively the linear chromaticities. h_{20001} and h_{00201} drive half integer (synchrobetatron) resonances ($2\nu_x$, $2\nu_y$) for off energy particles and thus excite the momentum dependent beat of beta functions [2], leading to a restriction of longitudinal acceptance. h_{21000} and h_{10110} drive the integer (ν_x), h_{30000} the third integer ($3\nu_x$), and h_{10200} and h_{10020} the coupling resonances ($\nu_x \pm 2\nu_y$), leading to a restriction of transverse acceptances.

The rank problem

With the N_{sext} sextupoles grouped into M_{sext} families, the nine equations form a $9\times M_{sext}$ linear system, since they are linear in sextupole strengths:

$$\begin{pmatrix} \ddots & \vdots & \iddots \\ \cdots & \sum_{n \in M_m} \beta_{xn}^{\frac{j+k}{2}} \beta_{yn}^{\frac{l+m}{2}} \eta_n^p e^{i\{(j-k)\mu_{xn}+(l-m)\mu_{yn}\}} & \cdots \\ \iddots & \vdots & \ddots \end{pmatrix}_{9\times M_{sext}} \bullet \begin{pmatrix} \vdots \\ (b_3 l)_m \\ \vdots \end{pmatrix}_{M_{sext}\times 1} = \begin{pmatrix} \vdots \\ \sum_{n}^{N_{quad}} (b_2 l)_n \ldots . \\ \vdots \end{pmatrix}_{1\times 9}$$

In principle, this system can be solved for the M_{sext} dimensional vector of sextupole strengths in order to eliminate all nine terms in one step. Of course, an exact solution requires rank 9 of the matrix. To fulfil this rank condition is difficult in high brightness light source lattices where the horizontal phase advance per cell usually is close to 0.5 (180°), so that the h_{20001} mode becomes directly proportional to h_{11001} (linear chromaticity) due to $e^{i2\Delta\varphi} \approx 1$ (i.e. the $2\nu_x$ mode is amplified coherently by all the sextupoles), and the linear system degenerates down to rank 8. In this case no feasible sextupole pattern exists to eliminate both h_{20001} and h_{11001}! – Of course, the problem could be solved elegantly as well as thoroughly by avoiding phase advances between sextupoles and quadrupoles, i.e. by incorporating the sextupoles into the

quadrupoles and setting their strength to $b_3 = b_2/\eta$. But this is impossible if there is zero dispersion somewhere in the lattice, and further would not allow any flexibility of the lattice.

Cancellation by phase

The only possibility to treat h_{20001} is to return to the linear lattice design and tune the optics in such a way, that the h_{20001} mode (and preferably maintaining the cancellation of the other modes) cancel by appropriate differences in betatron phase between sections of the lattice.

In multicell structures cancellations can be found for particular values of tunes per cell and number of cells. For example with $\Delta\nu_x = 0.4$ and $\Delta\nu_y = 0.1$ per cell all modes would cancel over five cells. This scheme was pursued in early versions of SLS [1]. However the contributions from the straight section quadrupoles and a necessary increase of cell tune in order to achieve the desired brightness lead to an incomplete cancellation and with it to restricted performance.

Later this problem was overcome by introducing phase trombones [2] that allowed cancellation between two arcs of the lattice over a wide range of operation of $\Delta\nu_x = 0.40...0.48$. However, the lattice became quite complicated and the longitudinal acceptance of approx. ±4% for different operation modes was considered to be still insufficient.

In the 12 TBA lattice the ideal phase cancellation scheme would adjust each TBA (including the halves of the adjacent straights) to $\Delta\nu_x = 7/4$ and $\Delta\nu_y = 3/4$ (which would be quite convenient choices to achieve low emittance *and* small beta functions in the straight sections) in order to cancel the h_{20001} and h_{00201} modes between 2 TBAs. The 5 geometric modes (ν_x , $3\nu_x$, $\nu_x \pm 2\nu_y$) would cancel between 2 TBA-pairs, because these are now apart by half an integer in tune.

Of course these ideal values for the tunes must not be used exactly in order to maintain closed orbit stability. Moreover, since the straights on both ends of a TBA are of different kind and thus their matching quadrupoles contribute differently to the chromatic modes, the best cancellation usually is found near, but not at the ideal tunes.

The final SLS lattice in both modes also works with a modified phase cancellation scheme based on one sixth (instead on one twelfth) of the lattice, using tune advances near $\Delta\nu_x = 13/4$ and $\Delta\nu_y = 5/4$ for 2 TBAs including the adjacent half straights and the full straight between. This leads to a slightly more relaxed lattice than the previous version.

Second order optimisation

Up to now these considerations concerned only the perturbations of first order in sextupole strength. However second order terms (sums over $(b_3l)_i \cdot (b_3l)_j$) corresponding to crosstalk between the sextupoles, are responsible for amplitude dependent tune shifts, second order chromaticity, second order dispersion and octupole like modes driving $2\nu_x$, $2\nu_y$, $4\nu_x$, $4\nu_y$ and $2\nu_x \pm 2\nu_y$ resonances. Suppression of first order terms is a necessary first step in suppressing the second order terms.

The derivation of analytical formulae for the second order terms is facilitated by Lie algebraic and computer algebra techniques [5] and gives lengthy but explicit and straightforward programmable functions of sextupole strengths, to be treated by a numeric minimisation procedure.

Eventually some skill in setting weight factors for the many terms, developed by systematic phenomenological studies, results in high brightness lattices with large longitudinal and transverse acceptances.

2.2.4 The ideal lattice: modes and performances

For discussion of the optics of the ideal lattice we may consider one periodic cell, corresponding to one third of the ring or 4 TBAs including one long, one medium and two short straight sections:

DL/2 – TBA – DS – TBA – DM – TBA – DS – TBA – DL/2

As long as only the ideal lattice, i.e. the lattice without magnet errors and RF cavities is concerned, all considerations may be based on this structure, i.e. one period, since in the ideal lattice an assumed particle does not „know“ that the ring is closed but only „sees“ repetitions of the same period.

General considerations on the lattice tune

Every bending magnet in a low emittance lattice and every straight, in particular a mini-beta straight, has a sharp beam waist. With $\Delta\nu_x = 0.5$ the maximum tune advance asymptotically achievable over a beam waist the horizontal tune of one period (4 straights and 4 TBAs with each 3 bending magnets) has an upper limit of $\nu_x = 8.0$. In order to achieve low emittance, this boundary has to be approached on a 85...90 % level. This was also done in the previous design, proposing to operate at $\Delta\nu_x = 0.42...0.48$ over one cell of the 7BA [2]. Thus we expect for the standard mode of operation in the TBA lattice a horizontal tune in the range of $\nu_x \approx 7.0$ per period. The vertical tune is free.

Explanation of tables and figures

The performance data for the three lattice modes D0, D1, D2A are given in table t22_a:

- circumference of full lattice,
- natural horizontal emittance (effective emittance in brackets),
- beta function and dispersion in the centres of the straights and their maximum values in the lattice,
- tunes and linear chromaticities and the ratio of chromaticity over tune since this provides a measure for the strain of the optics,
- momentum compaction factor, energy loss per turn without insertion devices (same for all lattice modes), relative r.m.s. energy spread and damping times,
- transverse and longitudinal dynamic, geometric and combined acceptances with

– the dynamic acceptances from tracking (assuming infinitely wide beampipes), see figures f22_e, _j. (these values depend on the number of turns tracked and thus are not very precise),

– the geometric acceptance from the beampipe (assuming a perfectly linear lattice), simply given by $A = R^2/\beta_{max}$ with R the beampipe radii of $R_x = 32.5$ mm and $R_y = 17.5$ mm[1] (see section 2.6 on the vacuum system), and

– the combined acceptance from tracking with the finite beampipe width.

– The longitudinal acceptance is the TRELMA as defined above.

[1] Update: Vertical aperture has been changed to $R_y = 16$ mm, however the plots are still for $R_y = 17.5$ mm

- Maximum quadrupole and maximum integrated sextupole strength.

The figures f22_c and f22_d display the linear optics of half a period of the lattice in D0 and D1 mode.

Figure f22_b is a tune diagram showing the location of the working points.

The non-linear performance of the lattices, i.e. the dynamic apertures and momentum acceptances as seen from the centre of the long straight section and the variation of tune shifts with amplitude and with momentum are displayed in figures f22_e – h for the D0 mode and in figures f22_j – m for the low emittance mode. For the D0-mode also the TRELMA as a function of beampipe width is shown in figure f22_i.

Description of the D0 mode (old standard mode)

The standard mode of operation with no dispersion in the straights and low emittance exploits the phase cancellation scheme as explained on the base of 1/12 of the lattice horizontally and on the base of 1/6 of the lattice vertically. The horizontal tune advance was adjusted to $\Delta\nu_x = 1.73$ for the first cell to be seen in figure f22_c (`DL/2-TBA-DS/2`) and to $\Delta\nu_x = 1.74$ for the second cell (`DS/2-TBA-DM/2`), close to the ideal value of $\Delta\nu_x = 7/4$. Verticlly both cells together have a tune advance of and $\Delta\nu_y = 1.18$, which is reasonably close to $\Delta\nu_y = 5/4$, providing cancellation of the $2\nu_y$–modes with the mirror image of the two cells shown.
This measure successfully suppresses the off momentum half integer resonances and with it the momentum dependent beat of beta functions and the second order chromaticity as to be seen from figure f22_h. The dynamic apertures are much larger than the beam pipe as to be seen from figure f22_e. The amplitude dependant tune shifts are rather flat and avoid major resonance crossings (figure f22_f). The momentum acceptance from tracking with beam pipe limitations is shown in figure f22_g: Obviously the beam pipe defines the acceptance rather than the dynamic stability limit. This becomes even more clear from figure f22_i showing the linear and nonlinear TRELMA as a function of beampipe width. (On variation of momentum acceptance along the lattice see [7].)

Description of the D1 mode (low emittance)

In a distributed dispersion lattice, i.e. by allowing dispersion in the straight sections, the emittance can by lowered further, since the end bending magnets, usually producing a factor 3 larger emittance than centre bending magnets now have an optics like centre bending magnets with $\eta' = 0$ approximately in the middle as to be seen from figure f22_d. A lower emittance of 3.85 nm is achieved at 2.4 GeV, in the long [medium, short] straight appearing as an effective emittance of 4.02 [4.10, 4.14] nm due to the finite dispersion leading to a contribution from energy spread beam widening.
Due to distributed dispersion all sextupoles act now on the chromatic terms, and this results in the matrix for the first order sextupole modes suppression not to become degenerate like it does in the lattices with dispersion free straights with only three chromatic sextupole families. Basically it thus would not be necessary to suppress the half integer modes by phase cancellation, however the lattice in D1-mode still has rather small dispersions and best solutions were found when still following the phase cancellation scheme. Here cancellation is exploited on the base of 1/6 of the lattice horizontally and vertically. The tunes of the lattice structue shown in figure f22_d were adjusted to $\Delta\nu_x = 3.205$ and $\Delta\nu_y = 1.26$, close to the ideal $\Delta\nu_x = 13/4$ and $\Delta\nu_y = 5/4$ for cancellation with the mirror image of the structure shown.
By 15% lower effective emittance and even slightly larger acceptances (figures 22_j-_m) make the D1-mode an interesting alternative to the standard D0-mode, if the complications from dispersion in the range of 5...8 cm in cavities and undulators can be handled.

Description of the D2A mode (low coupling)

The D0 lattice with its vertical tune of 7.08 turned out to be rather sensitive to misalignment errors and thus did not allow to lower the emittance coupling to 1% (see below). The D2A lattice has the vertical tune moved to 8.28 with phase advances of 0.69/TBA, allowing coupling down to 0.25 %. However this is on the expense of dynamic aperture, which is still larger than the geometric aperture but inferior to the D0 mode. This lattice mode leaves room for further optimization.

2.2.5 The real lattice

Girder arrangement

Groups of magnets will be mounted on girders, fixed by a precisely machined groove without further adjustment possibilities. The girders are connected by joints between adjacent girders, forming a closed polygon, the so-called „train link“ (see section 7 on alignment). The joints between the girders could be virtual, e.g. by means of optical or mechanical alignment systems, even over the straight sections. The joints will be located underneath the bending magnets with the bending magnets supported by two different girders as sketched here:

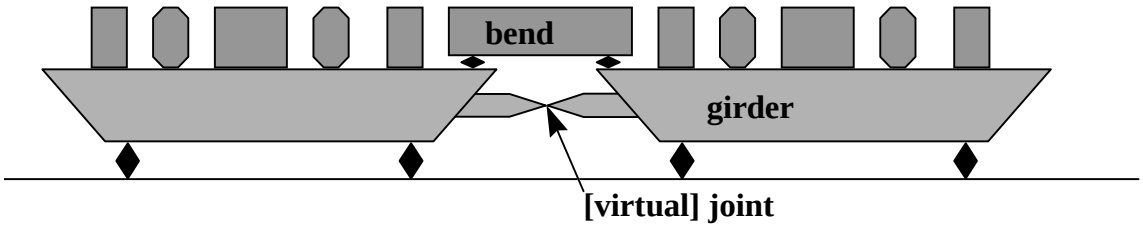

Clearly the transition from one girder to the next should occur at a location where the beta functions are small, i.e. where the divergence of the beam is large and thus a kink in the magnetic axis excites only a small betatron oscillation of the closed orbit. This is well fulfilled in the horizontal, since the horizontal betafunctions are smallest ($\beta_x \approx 0.3$ m) at the bending magnet centers which is the location of the girder joints. In the vertical the location is not ideal, but since β_y is rather large everywhere much better locations would not be available anyway (see figures f22_c, _d).

We now have to consider three kinds of misalignments:

- Displacement of the girder joints
- Play inside the girder joint
- Displacement of the magnets relative to the girder

The sensitivity of the closed orbit relative to these different kinds of misalignments is expressed by the so called amplification factors, defined as the ratio of the r.m.s. closed orbit at every lattice location (not only at BPM locations) and the r.m.s. girder displacements, averaged over a large number of random seeds. In principle the closed orbit is a nonlinear function of displacement due to sextupole contributions, however these contributions are largely suppressed after extermination of the integer resonance driving sextupole modes by proper setting of sextupole strengthes for dynamic aperture reasons [6].

Averaging over 100 seeds the following amplification factors a_x and a_y were found:

Error source	a_x	a_y	
		D0 mode	D2A mode
Girder joint misalignment	6	10	3
Girder joint play	22	10	4
Element misalignment relative to girder	58	69	25

Girder joint and joint play calculations were done for 100 μm r.m.s (maximum 200 μm = 2σ) displacements. Elements misalignment calculations were done twice for 10 μm and 50 μm r.m.s. (maximum 2σ) displacements with almost identical results (within 5%) proving that the sextupole influence is negligible.
Moving the tune from 7.08 (D0) to 8.28 (D2A) improved the vertical amplification factors by a factor 3 corresponding to the $1/\sin(\pi\nu)$ term in the closed orbit formula [6].

Figure f22_n shows histograms for the D0 mode for the r.m.s. closed orbit distortion from 100 seeds assuming a very well aligned situation with 100 μm r.m.s (maximum 2 σ) horizontal and vertical displacement of the girder joints, 10 μm r.m.s (maximum 2 σ) internal play of the girder joints and 30 μm r.m.s (maximum 2 σ) horizontal and vertical displacement of the elements on the girder. The locations of girder joints and beam position monitors can be seen from table t22_b (marked by underlined and *italic* font resp.).
The average r.m.s. closed orbit distortion from the combination of the three error sources with different amplification factors amounts to

$$\langle\sigma_x\rangle = 1.84 \text{ mm and } \langle\sigma_y\rangle = 2.33 \text{ mm},$$

which is exactly what one would expect from quadratic addition.

Proposed BPM and corrector layout

As a low emittance light source SLS performance is limited by non-linear effects, i.e. restrictions of dynamic acceptance and with it life time due to additional focusing from the sextupoles, seen by the closed orbit distortions due to magnet misalignments. Therefore beam position monitors are placed close to the sextupoles, since correction of the orbit will then restore the linear optics and hence the symmetry of the lattice. Most of the orbit correctors are also located at the sextupoles, physically as additional coils.
Each 72 beam position monitors and combined horizontal and vertical correctors were used. Thus 40 from the 120 sextupoles would be equipped with correction coils. This concerns the sextupole families `SE, SD` inside the achromat and the families `SLB`, `SMB`, `SSB` in the matching sections to the straights.

Sensitivity to alignment errors

Figures f22_q and f22_r show for the lattice in D0 mode and in D1 mode the sensitivity of dynamic acceptance on the displacement errors. Due to the philosophy of correcting the orbit in the sextupoles the acceptances appear to be rather robust.

Real lattice performance

Figure f22_s shows for the D0-mode of the lattice the results for the transverse acceptances as a function of relative energy deviation for the error free lattice and for a 200 μm r.m.s. girder, 10 μm r.m.s. girder joint play and 30 μm r.m.s. magnets misalignment with following orbit correction, using 72 horizontal and vertical beam position monitors and correctors. Tracking was done without synchrotron oscillations. Closed orbit correction largely restores the

acceptances of the ideal lattice. Finite acceptances exist in a range of ±6%, with the limitation given by the half integer stopband $\nu_x = 20.5$ (see figure f22_h).
Figure f22_t shows the same calculations for the D1-mode of the lattice. Finite acceptances exist in a range of ±6%, with the limitation given by the integer stopband $\nu_x = 19$ (see figure f22_m). With lower effective emittance and even larger acceptances the D1-mode seems to be the preferable mode of operation if there is no unexpected increase of energy spread from single or multi-bunch instabilities.

2.2.6 Beam Dynamics issues addressed recently[2]

Beam Dynamics Software Development

1. The PASCAL code TRACY-2 [9] has been ported to C [10] in order to provide a flexible beam dynamics software library on a PC platform which is capable of doing the calculations needed for the development of a realistic machine model and the control of the real machine. Several extension to the library have been made including routines for the calculation of betatron coupling and generalized sigma matrices [11].
2. A PC based Beam Dynamics Group Server (`slsbd.psi.ch`) running LINUX has been configured which keeps accelerator physics specific information and tools at a central location. This simplifies the communication between group members and provides them with a standardized working environment. Codes like the TRACY-2 library, MAD, IDL, SIXTRACK and the CERN libraries are kept there. Documentation on ongoing studies is published using a Web Service (URL: `http://slsbd.psi.ch/`) . Jobs can be submitted on the server utilizing an NQS service.

Beam Dynamics Calculations

1. The betatron and emittance coupling for distorted lattices has been estimated and possible correction schemes have been explored.The beam ellipse twist in the straight sections is calculated to be around40 mrad. The corresponding value for the emittance coupling in mode D1 is 0.2 % and 1 % in zero dispersion mode D0. This relatively large coupling factor for the latter mode can be explained by the fact that the verticalworking point has been chosen very close to the integer ($\nu_y = 7.08$) inorder to optimize the Dynamic Aperture (DA). This leads on the other hand to ansignificant increase of the spurious vertical dispersion. A change of the vertical tune to $\nu_y = 8.28$ leads to a reduction of the emittance couplingto 0.25 %. The remaining vertical dispersion of 0.3 cm is mainly induced by sextupoles. The contribution from quadrupoles is nicely compensated by the dispersion generated by the nearly adjacent orbit correctors. The contribution from the feeddown of horizontal dispersion via sextupoles remains. It turns out that this feeddown can be corrected using asymmetric orbit bumps in the arcs or better dedicated skew quadrupoles resulting in a residual coupling of less than 0.1 %.
2. Closed orbit correction schemes for slow (< 1 Hz) and fast orbit control (< 100 Hz) have been simulated and analyzed. For the present monitor and corrector layout (72 monitors and 72 correctors at the same locations in both planes) the single value decomposition (SVD) and the sliding bump orbit correction scheme converge to the same residual orbit. Rms values of about 200 μm (zero monitor readings) are observed in both planes. The maximum corrector kicks needed are well below (50 %) the design maximum of

[2] This section is new in the Oct 98 version of this chapter. It describes work done since March 98.

approx. 1 mrad (horizontal 0.98, vertical 1.13 mrad). In the vertical direction about 20 % more corrector strength is needed than in the horizontal plane although the horizontal rms kick is about 30 % larger than in the vertical. This can be explained by a 50 % less efficient correction in the vertical plane.The global SVD scheme has the advantage of being able to handle an unequal number of monitors and correctors in the case of faulty monitors and/or saturated correctors and is therefore much more flexible. On the other hand the SVD scheme requires a good knowledge of the entire linear machine optics in order to determine the appropriate inverse corrector-monitor correlation matrix A^{-1}. A^{-1} turns out to be a tridiagonal sparse matrix which explains why SVD and sliding bump scheme converge to the same correction state. The locality of A^{-1} has implications on the implementation of the fast global orbit feedback. 12 sectors consisting of 6 monitors and 6 correctors each have only to be able to acquire monitor data from their left and right hand neighbours in order to determine their corrector values (see also ``storage ring diagnostics" chapter 2.8.3.4.3.5).

3. The degradation of the DA has been calculated for multipole field errors based on field maps provided by the magnet manufacturerer. The integrated multipole content derived from 3-dim calculations for quadrupoles and sextupoles is acceptable as it was already shown in [8]. The vertical correctors with dipole coefficient b_1 which are integrated into the sextupoles create a large decapole component b_5. The ratio of the multipole coefficients b_5/b_1 is calculated to be $5.25 \cdot 10^5$ m^{-4}. Assuming a linear scaling of b_5 with b_1 the DA has been calculated for a large number of distorted and orbit corrected machines operated in the D0 lattice mode. It has been shown that the DA is only significantly reduced for large momentum deviations $dp/p > 2$ %.
4. Short and long term stability constraints and their influence on powersupply specifications have been analyzed.
5. First calculations on Beam Based Alignment (BBA) procedures have been performed. Foreseen are two basic modes of operation:
    a) Static Mode: the strength of a quadrupole is changed once and the corresponding difference orbit is measured. Additionally the beam position at the quadrupole location is varied with a local orbit bump.
    b) Dynamic Mode: the strength of a quadrupole is modulated with a few Hz and the orbit response is measured. A variant would involve an additional variation of the orbit at the location of the quadrupole. A vanishing orbit response would then indicate the zero crossing. In order to ensure a 1 μm resolution of the BBA procedure for all quadrupoles with adjacent monitors a peak to peak modulation of 5 % of the maximum integrated quadrupole strength $K = 1.12$ m^{-1} in D0 mode should be foreseen. At this amplitude modulation frequencies between 3 and 5 Hz would be compatible with the characteristics of the envisaged unipolar powersupplies (see also ``storage ring diagnostics" chapter 2.8.3.4.2). The mentioned quadrupole strength variation corresponds to a maximum betatron tune change of 0.08.

References

[1] Conceptual Design Report of the Swiss Synchrotron Light Source, PSI 1993

[2] J. Bengtsson et al., Status of the Swiss Light Source Project, in: Proc. EPAC 96, Sitges (Barcelona) 1996

[3] D. Einfeld and M. Plesko, A modified QBA optics for low emittance storage rings, NIM A 335 (1993) 402

[4] D. C. George and V. Vrankovic, 2D study of the SLS storage ring quadrupoles, SLS Note 3/95

[5] J. Bengtsson, The sextupole schemes for the Swiss Light Source (SLS): An analytic approach, SLS Note 9/97

[6] A. Streun, Reduction of closed orbit distortions by girders, SLS Note 10/93

[7] A. Streun, Momentum acceptance and Touschek lifetime, SLS Note 18/97

[8] L. Tosi and A. Streun, SLS dynamic aperture with minigap insertion devices, SLS-TME-TA-1998-0002

[9] J. Bengtsson, TRACY-2 User's Manual, February 1997.

[10] M. Böge, Update on TRACY-2 Documentation, July 1998.

[11] A.W. Chao, J. Appl. Phys. 50, 1979.

Tables:

Table t22_a: Comparison of the two lattice modes.

Geometric acceptance values assume an elliptic vacuum chamber with radii of 32.5 mm in the horizontal and 17.5 mm in the vertical.

Dynamic acceptance values are taken from figures f22_e, _j as squared dynamic aperture values divided by the local betafunctions. Due to nonlinear distortions of betatron motion this values differ significantly from acceptance values obtained from ellipse fits to a test particle's phase space motion like in figures f22_q, _r, _s or to acceptances taken as the squared amplitude of the limiting particle's fundamental peak in the Fourier spectrum divided by the local betafunction like in figures f22_f, _k.

For further explanations see text.

Lattice mode		**D0**	**D1**	**D2A**
Emittance @ 2.4 GeV (eff.. em.)	**nm·rad**	**4.80**	**3.85 (≈ 4.1)**	**4.81**
Circumference	m	288		
Long straight: β_x / β_y / η	m	4.1 / 6.1 / 0.0	13.7 / 6.5 / 0.08	4.3 / 3.0 / 0.0
Medium straight: β_x / β_y / η	m	1.8 / 4.3 / 0.0	3.5 / 4.0 / 0.05	1.8 / 2.5 / 0.0
Short straight: β_x / β_y / η	m	1.2 / 2.6 / 0.0	2.0 / 2.4 / 0.04	1.1 / 1.6 / 0.0
Maximum values: β_x / β_y / η	m	23.5 / 23.7 / 0.36	20.4 / 19.9 / 0.31	24.6 / 26.5 / 0.35
Tunes horizontal and vertical		20.82 / 7.08	19.23 / 7.56	20.82 / 8.28
Chromaticities hor. and vert..		-69.5 / -19.3	-56.2 / -17.2	-72.9 / -20.7
Ratio (chrom. / tune) hor. and vert.		-3.34 / -2.72	-2.92 / -2.27	-3.50 / -2.50
Momentum compaction factor	10^{-4}	6.56	6.42	6.56
Energy loss/turn (without IDs)	keV	512		
Natural relative energy spread	10^{-4}	8.58		
Damping times: hor. / vert./ long.	ms	9 / 9 / 4.5		
Hor. accept.: dyn. / geo. /combined	μm·rad	80 / 45 / 41	70 / 52 / 45	80 / 41 / 35
Vert. accept.: dyn. / geo. /combined	μm·rad	50 / 13 / 13	70 / 17 / 17	18 / 10 / 10
TRELMA: dyn. / geo. /combined	%	7.6 / 5.9 / 5.4	8.1 / 6.1 / 5.3	/ / 5.1
max.$\lvert b_2 \rvert$ in quad.	m^{-2}	2.27	2.50	2.54
max.$\lvert \int b_3 dl \rvert$ in sext.	m^{-2}	6.5	4.1	7.6

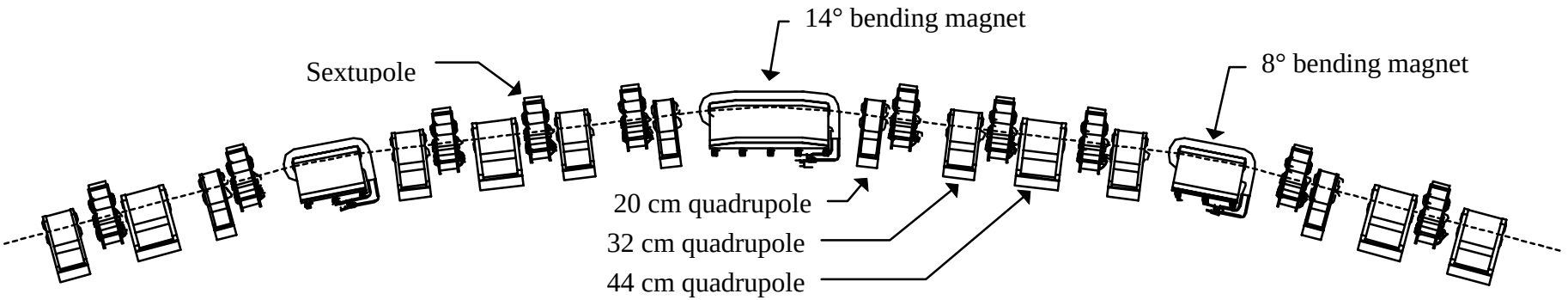

Figure f22_a: Layout of one TBA including matching to the adjacent straight sections

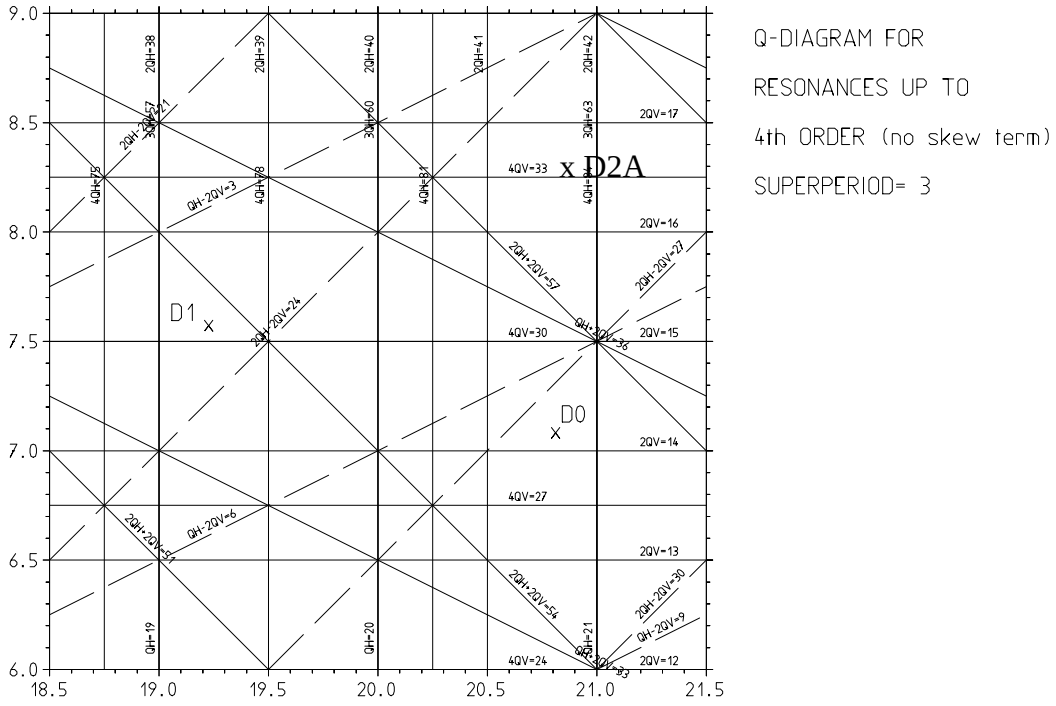

Figure f22_b: Tune diagram with the working points of the lattice in the 3 modes.

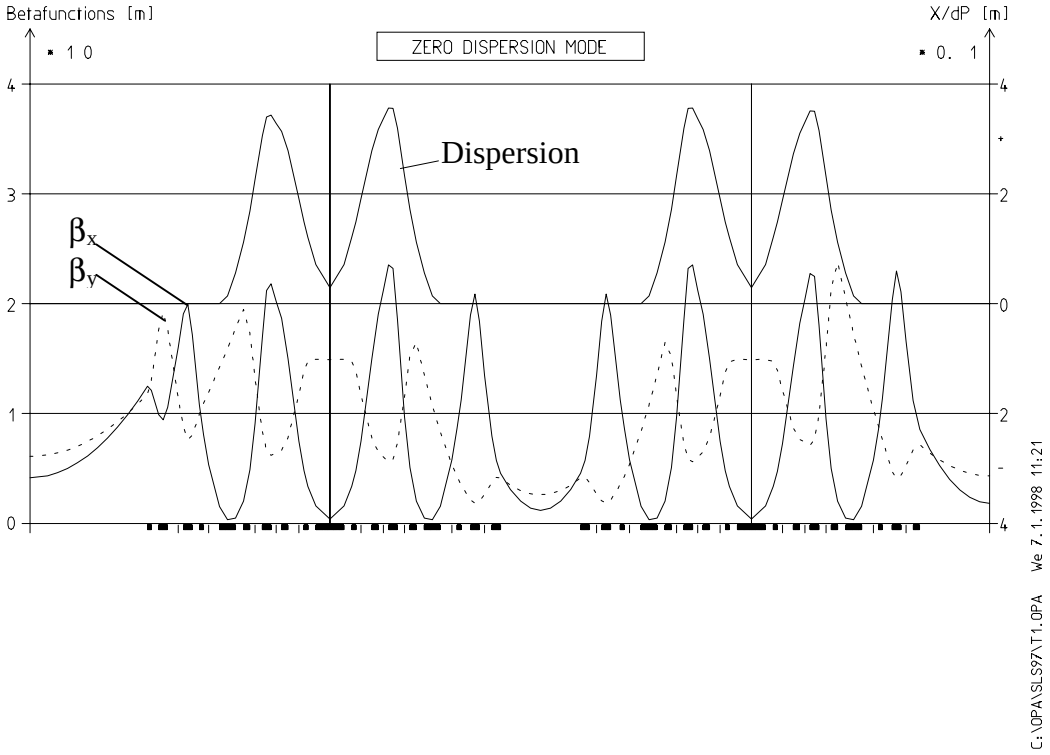

Figure f22_c: Optics of the D0-mode (standard), one sixth of the lattice is shown

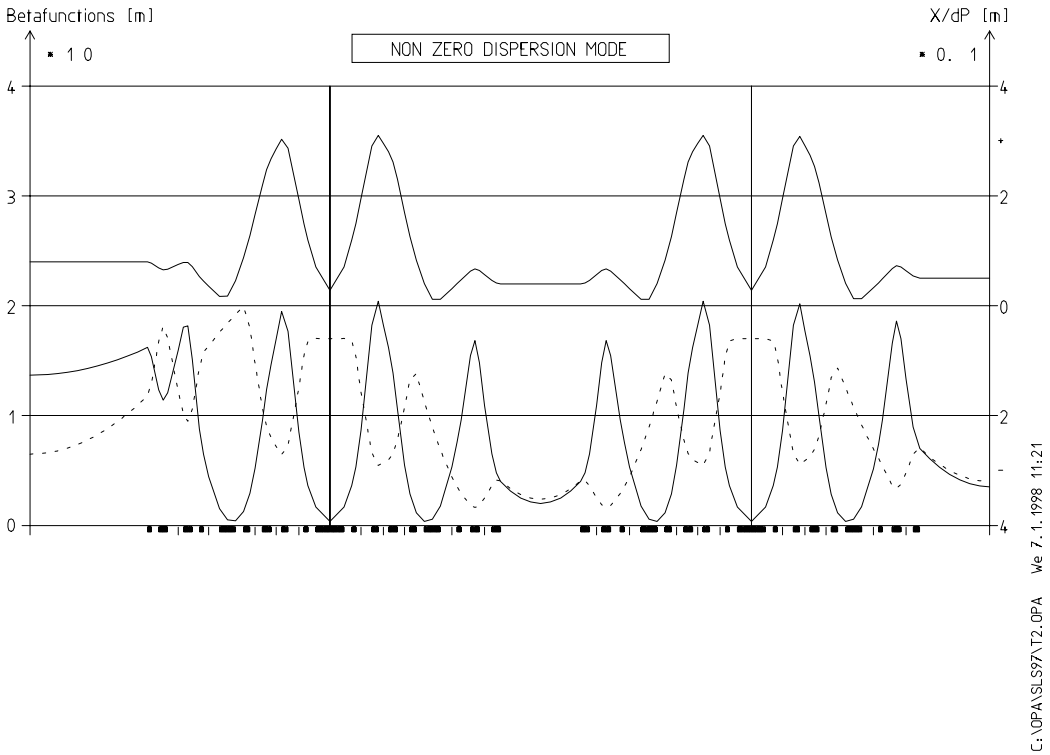

Figure f22_d: Optics of the D1-mode (low emittance), one sixth of the lattice is shown

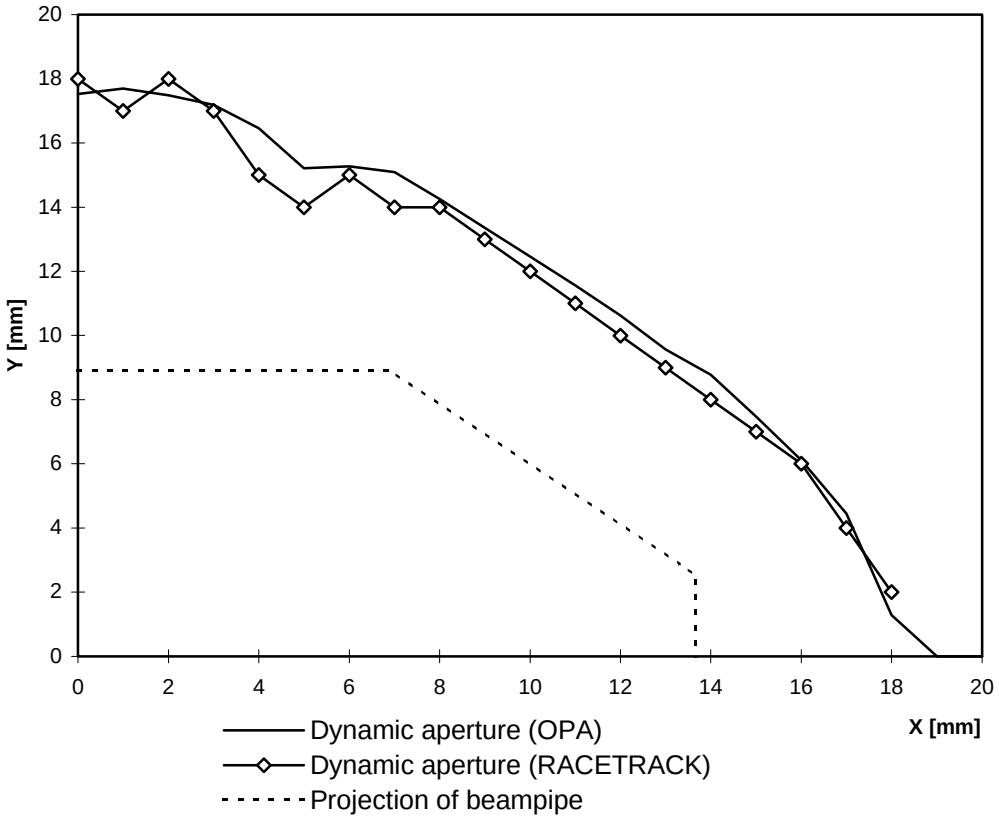

Figure f22_e: D0-mode: Dynamic aperture at the centre of the long straight. Since the aperture is asymmetric in the horizontal, the minimum from y(x) and y(–x) was taken. The OPA calculations were confirmed with the program RACETRACK [8]. The beampipe of 65 mm full width and 35 mm full height appears at the tracking point as shown by the dotted line.

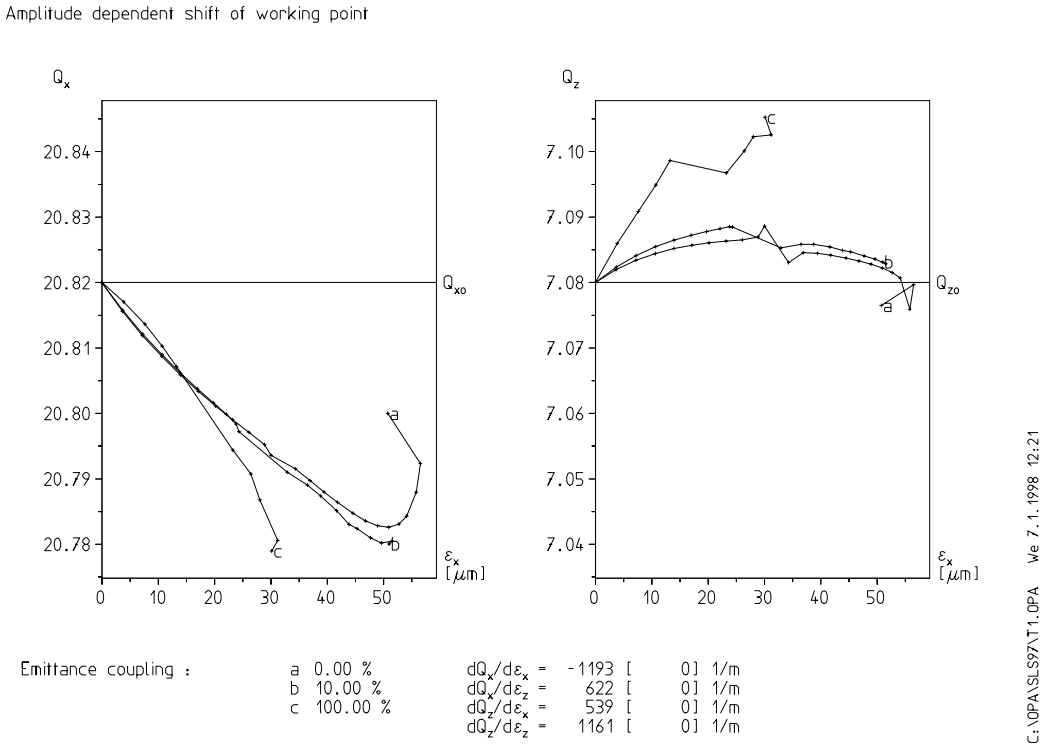

Figure f22_f: D0-mode: Amplitude dependent tune shifts from tracking (512 turns) and FFT. Betatron amplitude values were taken as the squared magnitude of the fundamental peak of the Fourier spectrum divided by the local betafunction. Close to the stability limit the dynamics becomes nonlinear, the amplitudes of higher harmonics increase on the expense of the fundamental betatron frequency and the curve „bends back“.

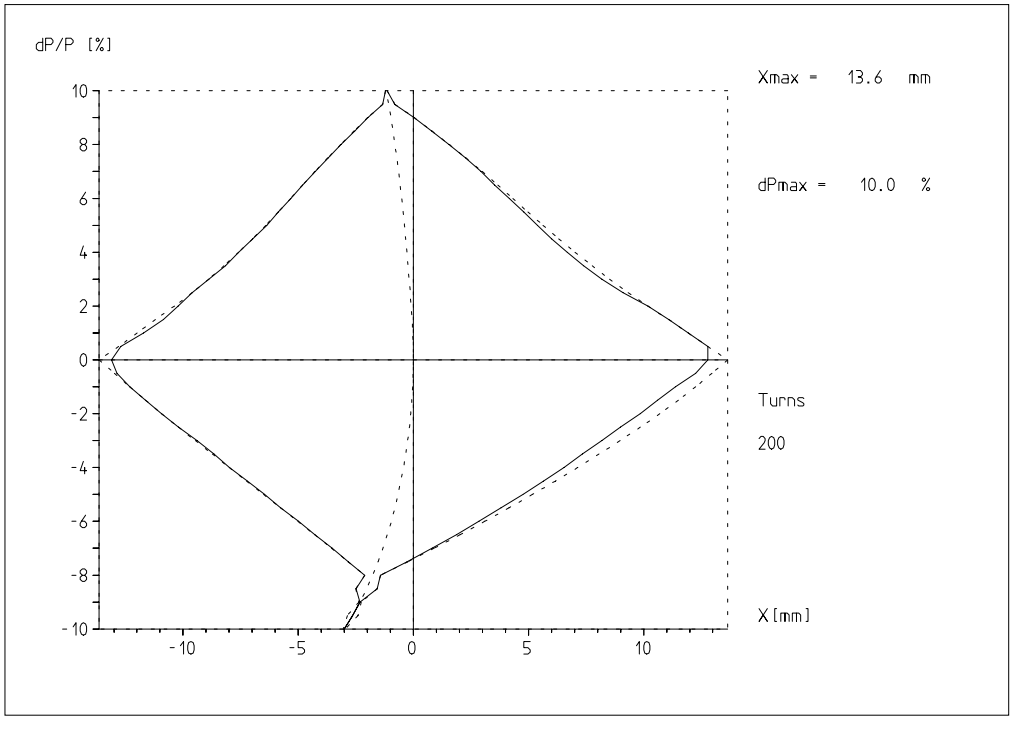

Figure 22_g: D0-mode: Momentum acceptance given by the horizontal aperture as a function of relative momentum deviation at the centre of the long straight section. Shown is the geometric aperture of the 65 mm wide beampipe (dotted) and the dynamic aperture within these geometric limits (solid). The central dotted line is the momentum dependant closed orbit. (OPA calculation)

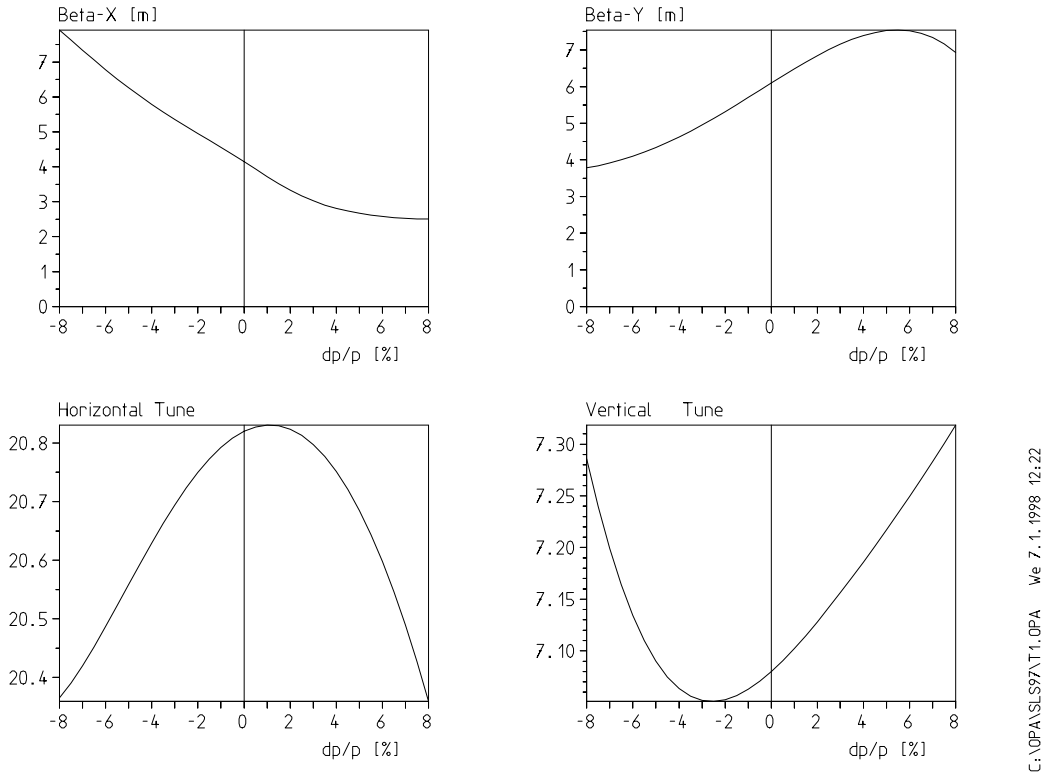

Figure 22_h: D0-mode: Momentum dependant betafunctions (long straight) and tunes

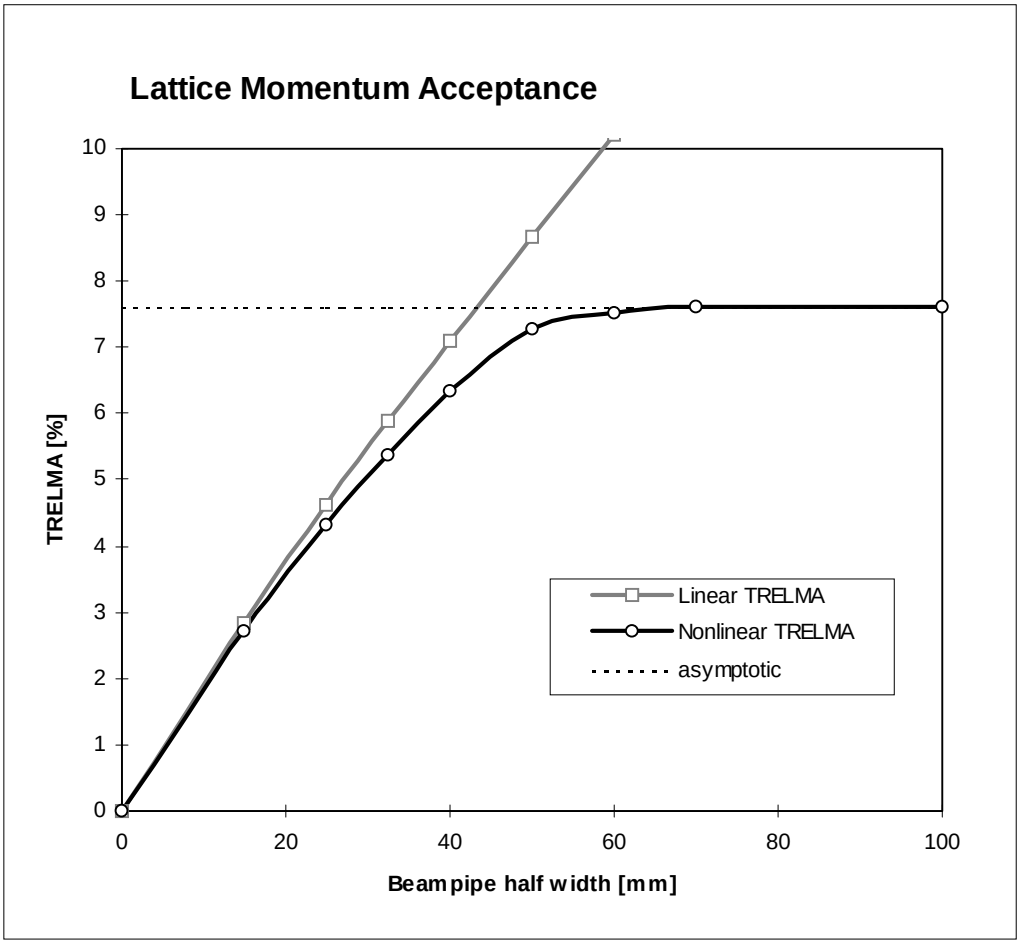

Figure f22_i: Linear and nonlinear TRELMA (Touschek relevant effective lattice momentum acceptance) as function of beampipe width for the D0-mode of the lattice.
At the proposed beampipe half width of 32.5 mm the lattice momentum acceptance is well within physical limitations.

The TRELMA is defined at that value of RF acceptance where where a calculation with only the RF acceptance (assuming infite lattice acceptances) and a calculation with only the lattice acceptance (assuming infinite RF acceptance) give the same result for the Touschek lifetime (normalised to bunch length) [7].
The linear TRELMA assumes a perfectly linear lattice without momentum or amplitude dependent distortions of orbit, tunes and betafunctions, and thus is defined by the beampipe width. The asymptotic value of the nonlinear TRELMA corresponds to the pure dynamical limitations of a lattice with infinitely wide beampipe.
(Momentum acceptance from binary search for maximum dp/p, resolution 0.02% in dp/p, 50 turns tracked) (OPA calculation)

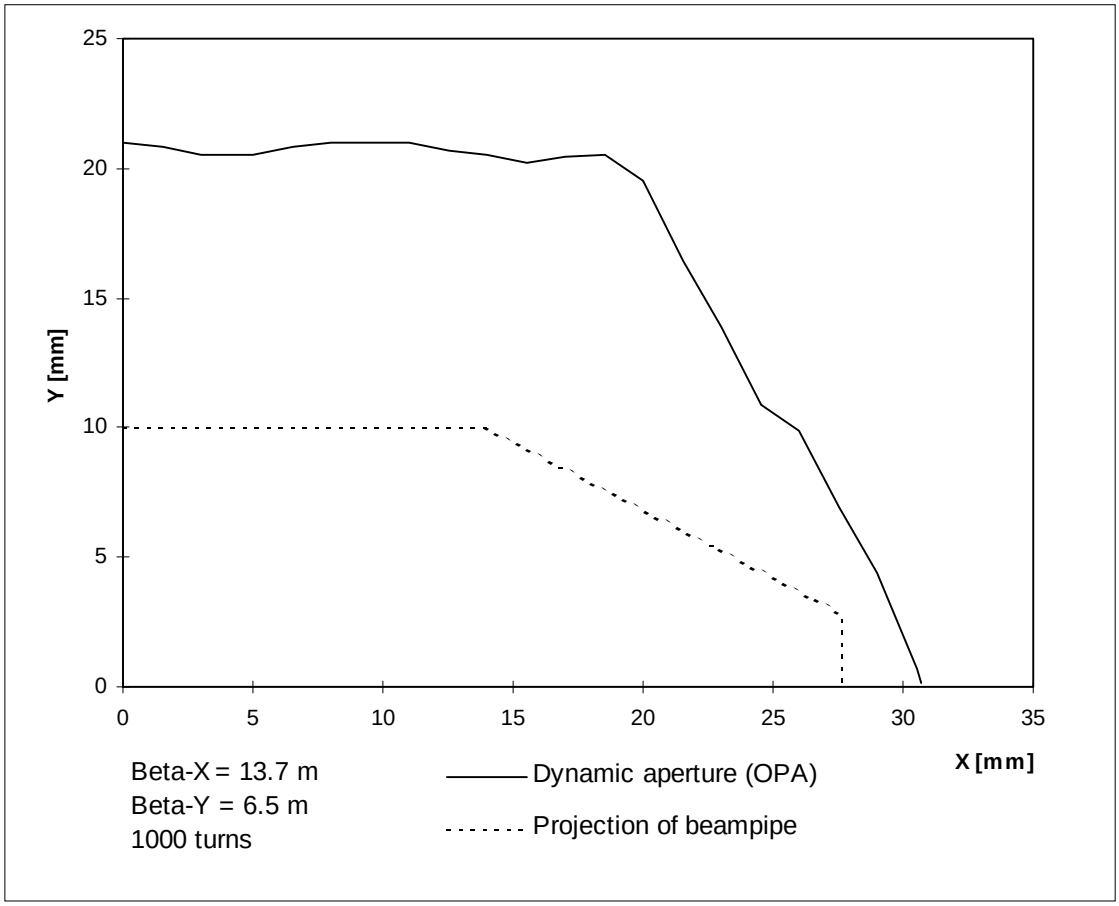

Figure f22_j: D1-mode: Dynamic aperture at the centre of the long straight. Since the aperture is asymmetric in the horizontal, the minimum from y(x) and y(–x) was taken. The beampipe of 65 mm full width and 35 mm full height appears at the tracking point as shown by the dotted line. (OPA)

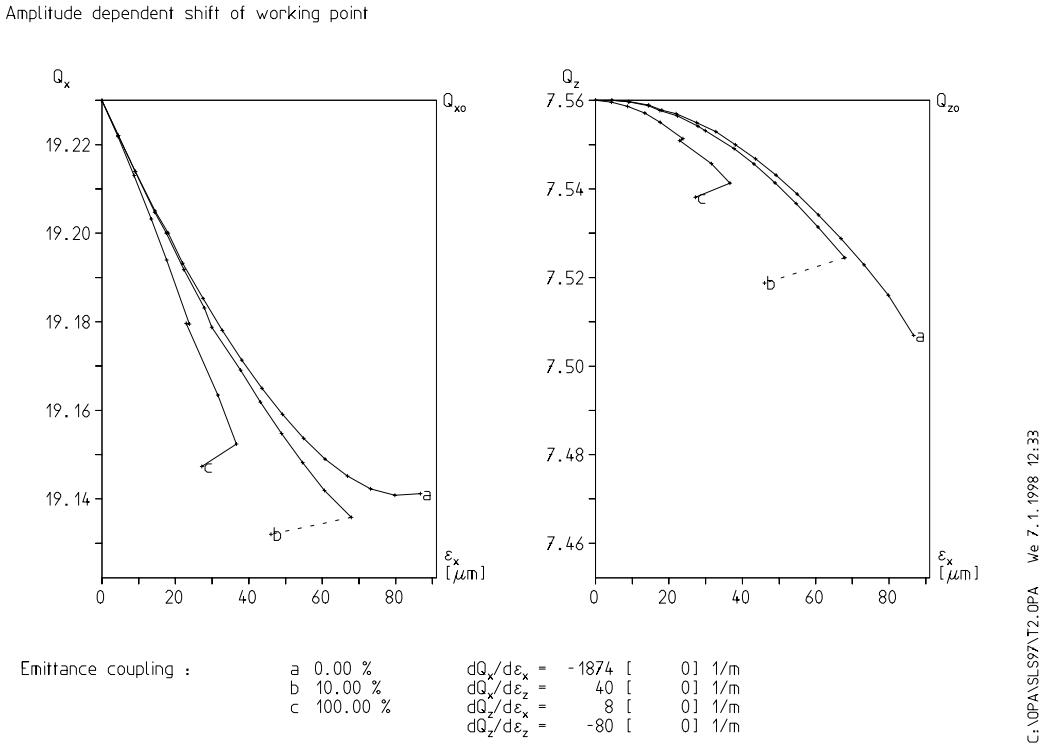

Figure f22_k: D1-mode: Amplitude dependent tune shifts from tracking (512 turns) and FFT. Betatron amplitude values were taken as the squared magnitude of the fundamental peak of the Fourier spectrum divided by the local betafunction. (OPA)

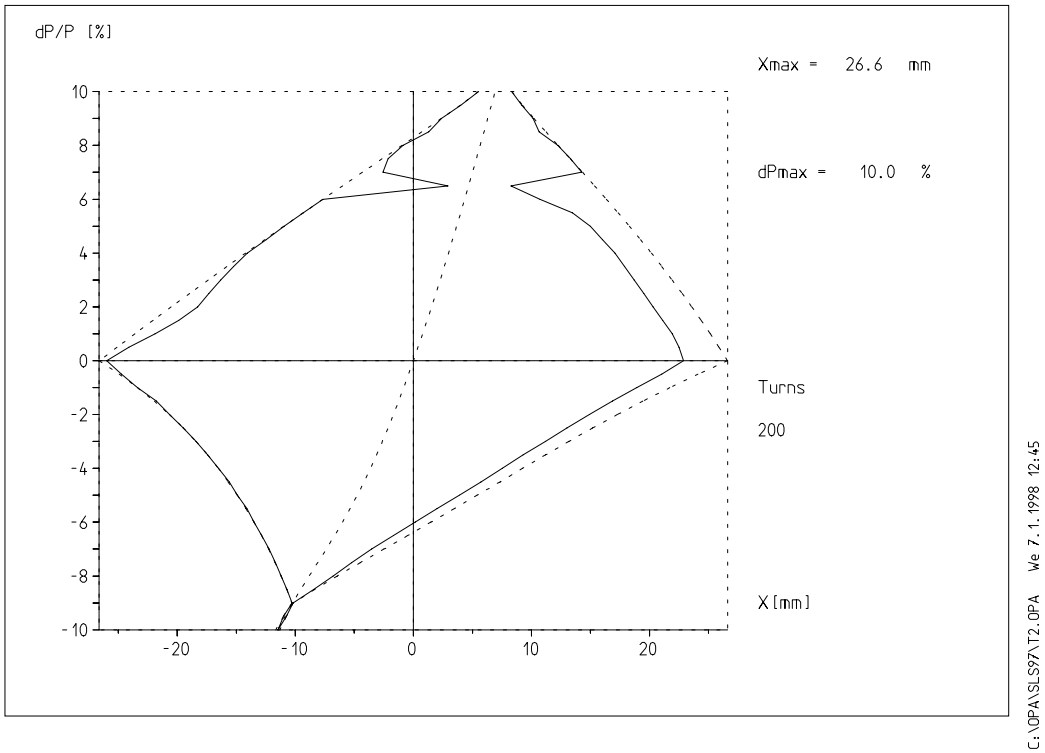

Figure 22_l: D1-mode: Momentum acceptance given by the horizontal aperture as a function of relative momentum deviation at the centre of the long straight section. Shown is the geometric aperture of the 65 mm wide beampipe (dotted) and the dynamic aperture within these geometric limits (solid). The central dotted line is the momentum dependant closed orbit. The breakdown at +6% corresponds to an integer crossing of the tune. (OPA)

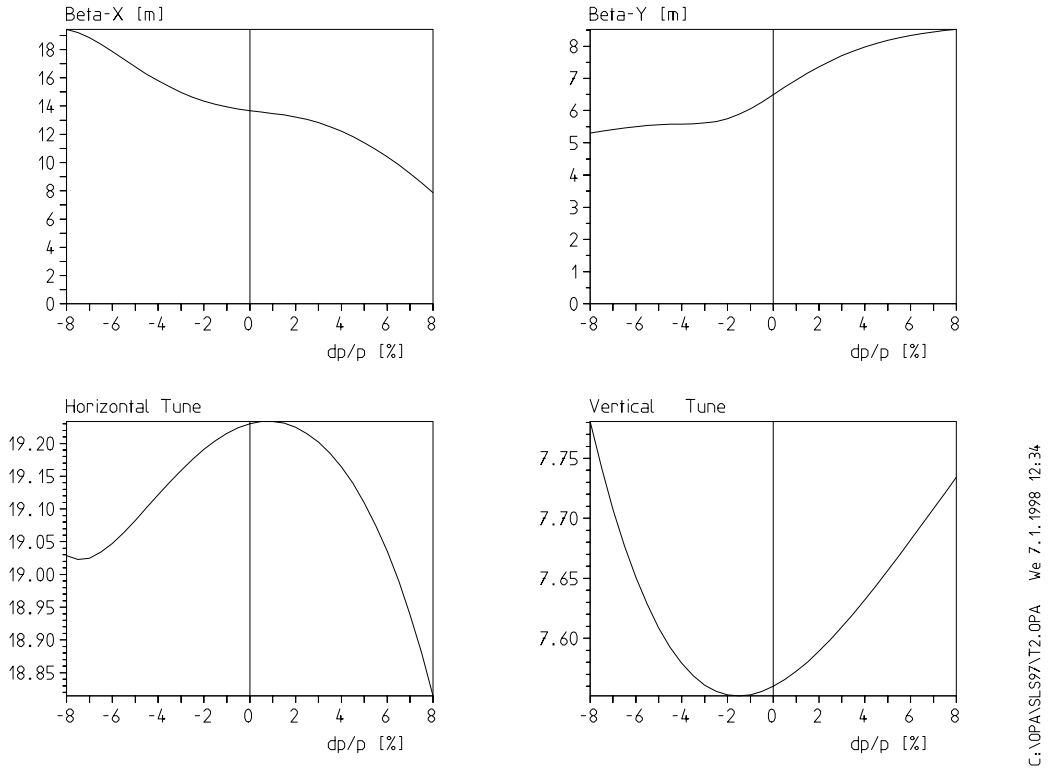

Figure 22_m: D1-mode: Momentum dependant betafunctions (long straight) and tunes (OPA)

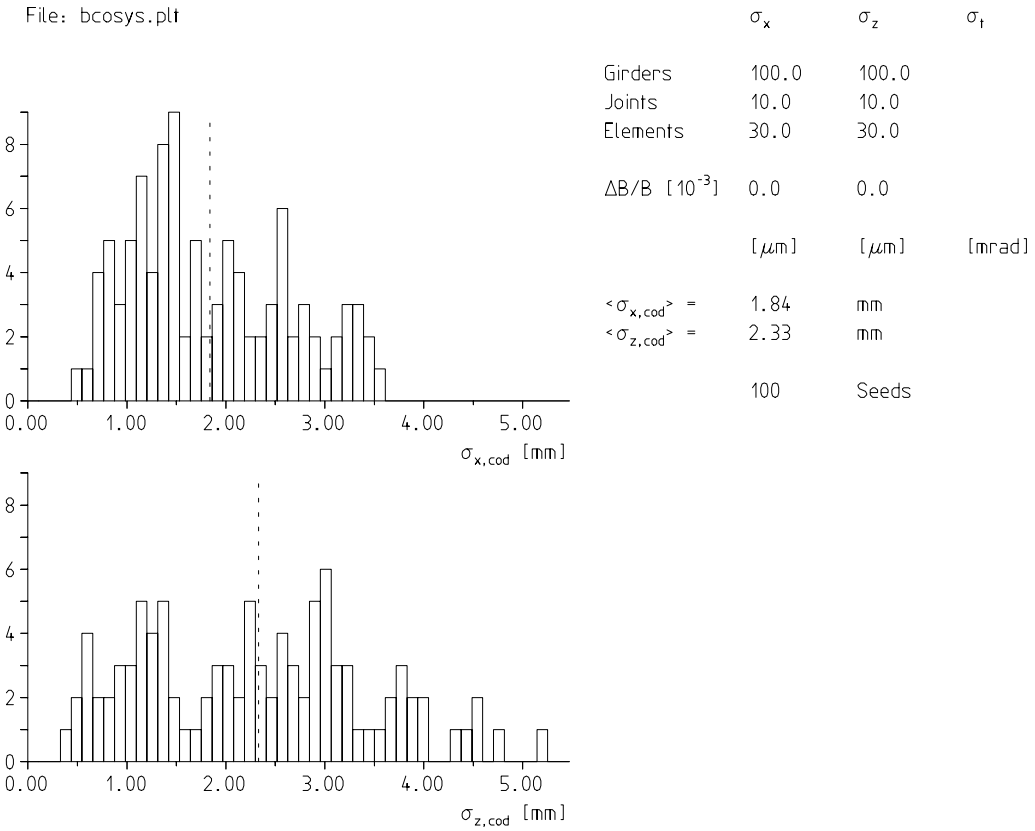

Figure f22_n: D0-mode: Histogramm of r.m.s. closed orbit distortions for 100 μm r.m.s. (cut at 2σ) displacement error of girder joints, 10 μm r.m.s. (cut at 2 σ) girder joint play and 30 μm r.m.s. (cut at 2 σ) displacement error of magnets relative to the girders (100 seeds).
(TRACY-2 calculation)

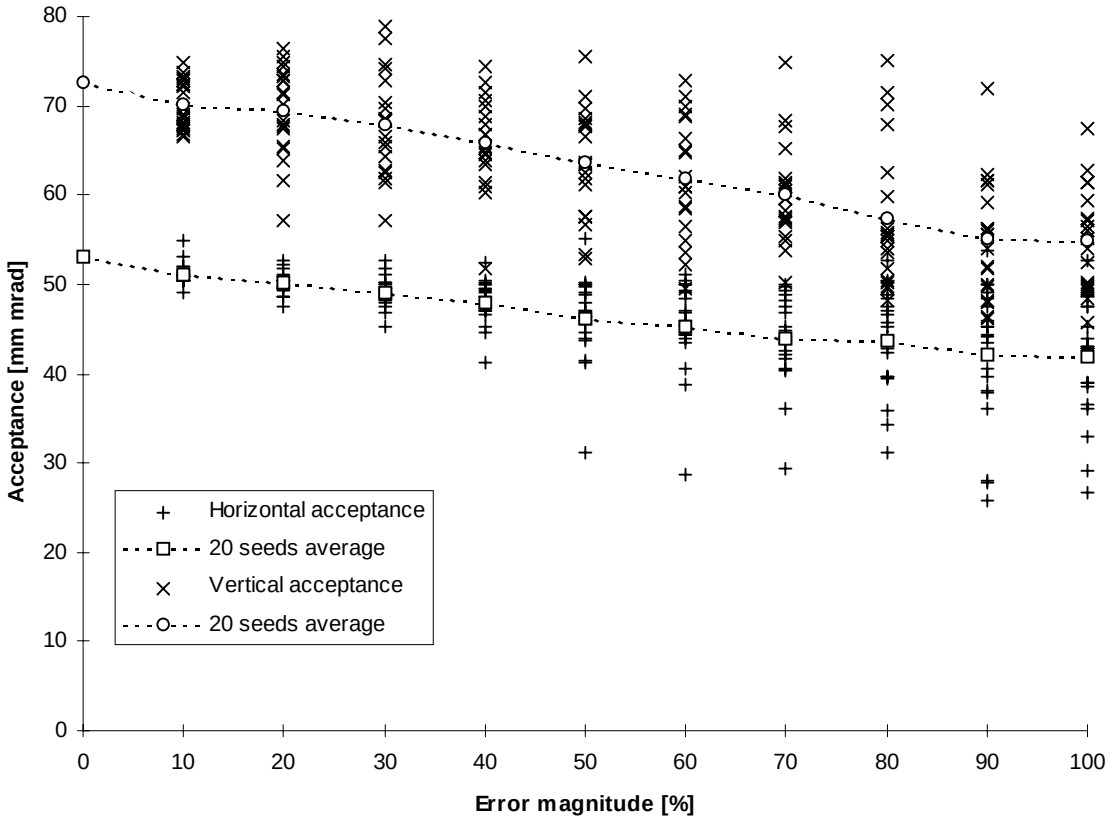

Figure f22_q: SLS in D0 mode (dispersionfree straight sections, see fig. f22_c)

Decay of dynamic acceptances with increasing error magnitude. 100% correspond to an r.m.s. (cut at 2 σ) error setting of 200 μm for the girder joints, 10 μm for the joint play and 30 μm for the elements relative to the girders. For each point the same set of 20 random seeds was used to set the misalignments.

The acceptance values were obtained from an ellipse fit to the Poincaré plot of the outermost stable particle's phase space motion as seen at the center of the long straight section. The outermost stable particle as a particle close to the separatrix of bounded motion was found by binary search (tracking 100 turns) for the starting coordinate x_o (with $x'_o = y'_o = 0$ due to symmetry, and $y_o = 10^{-6}\, x_o > 0$ in order to excite coupling resonances) for the horizontal and vice versa for the vertical acceptance. (TRACY-2 calculation)

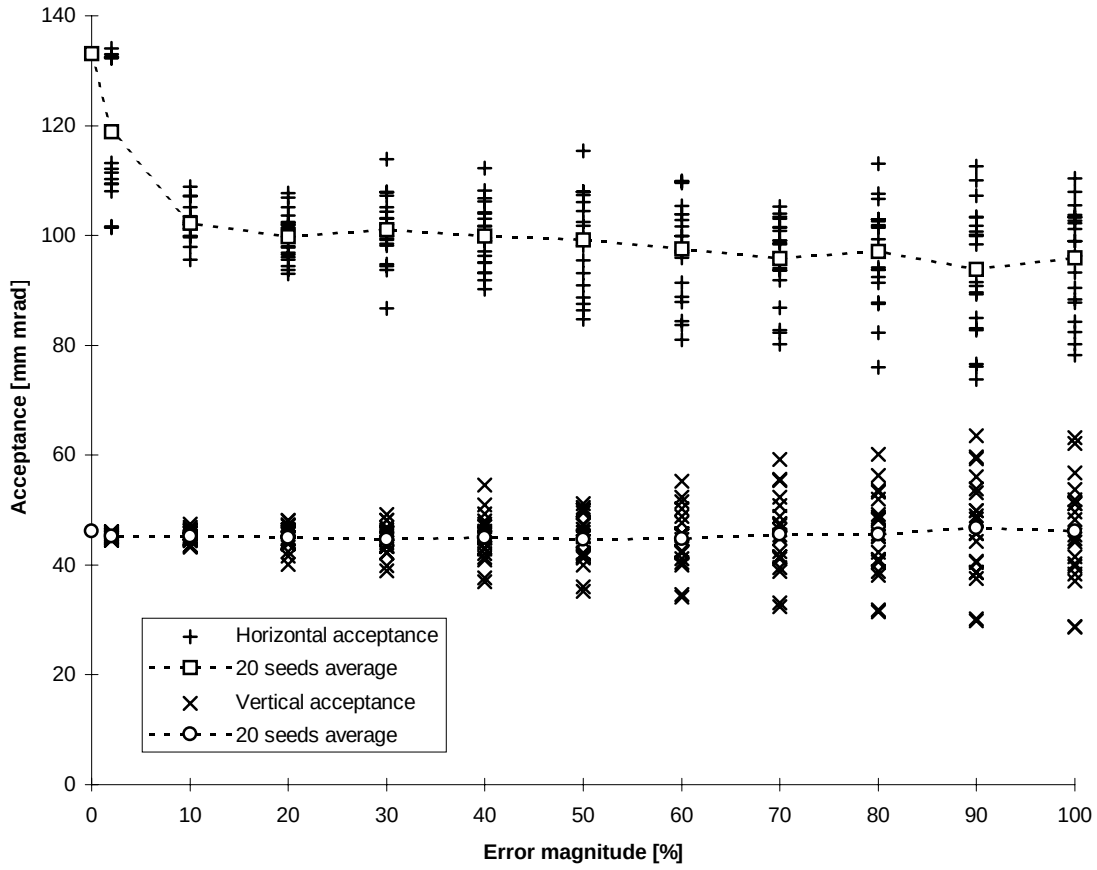

Figure f22_r: SLS in D1 mode (dispersive straight sections, see fig. f22_d)

Decay of dynamic acceptances with increasing error magnitude. 100% correspond to an r.m.s. (cut at 2 σ) error setting of 200 μm for the girder joints, 10 μm for the joint play and 30 μm for the elements relative to the girders. For each point the same set of 20 random seeds was used to set the misalignments.

The acceptance values were obtained from an ellipse fit to the Poincaré plot of the outermost stable particle's phase space motion as seen at the center of the long straight section. The outermost stable particle as a particle close to the separatrix of bounded motion was found by binary search (tracking 100 turns) for the starting coordinate x_o (with $x'_o = y'_o = 0$ due to symmetry, and $y_o = 10^{-6} x_o > 0$ in order to excite coupling resonances) for the horizontal and vice versa for the vertical acceptance. (TRACY-2 calculation)

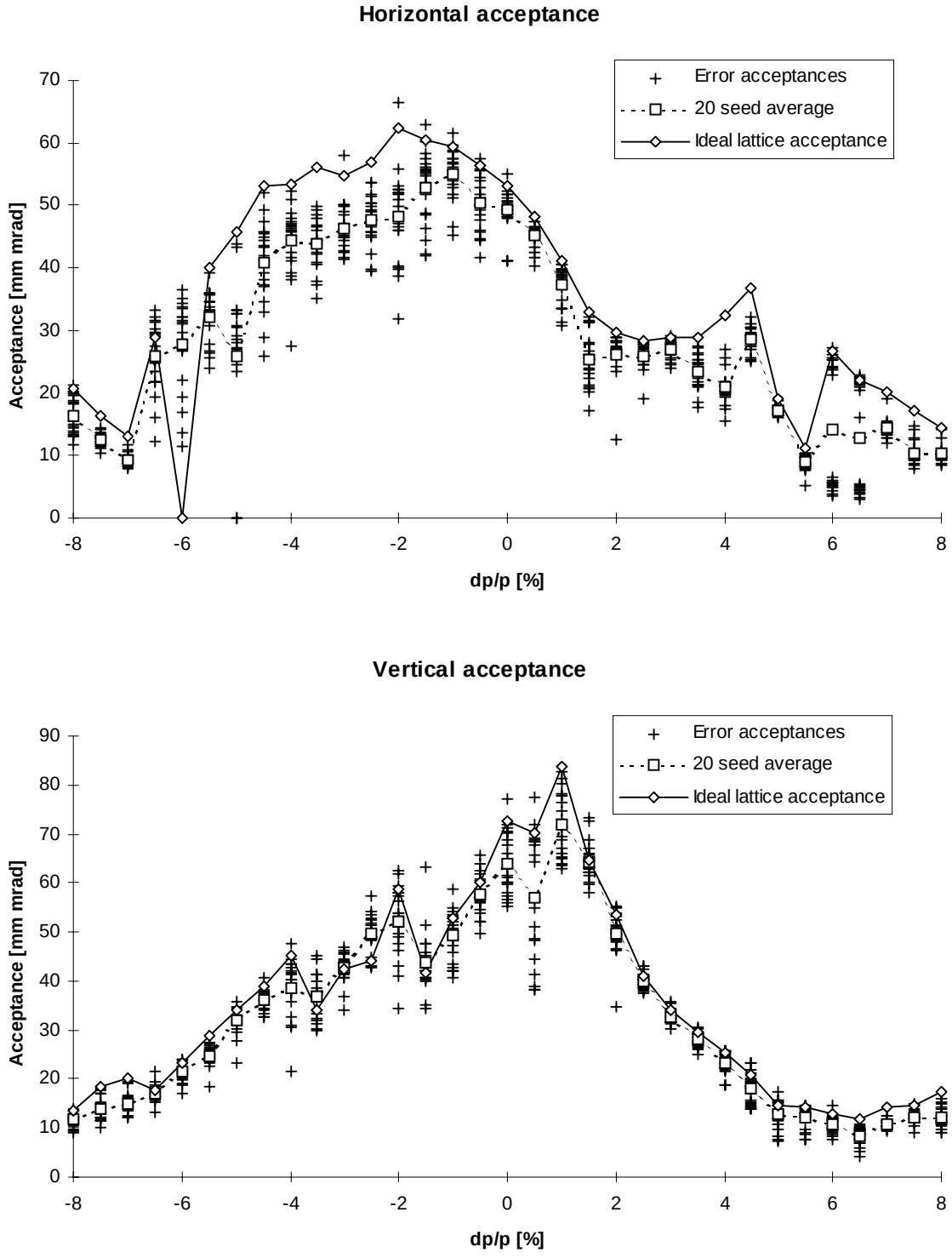

Figure f22_s: D0-mode: Horizontal and vertical dynamic acceptance as a function of relative momentum deviation for the ideal lattice and for the real lattice with displacement errors of 200 μm r.m.s. (cut at 2σ) for the girder joints, 10 μm r.m.s. (cut at 2σ) for the girder joint play and 30 μm r.m.s. (cut at 2σ) for the magnets relative to the girders (same set of 20 random seeds for every point). Displacement errors were also applied to the beam position monitors, sitting on the girders too. The closed orbit correction largely restores the acceptance values for the error free lattice. The breakdown for the horizontal ideal lattice acceptance at –6% is due to the momentum dependant tune crossing a half integer (see figure f22_h). (TRACY-2)

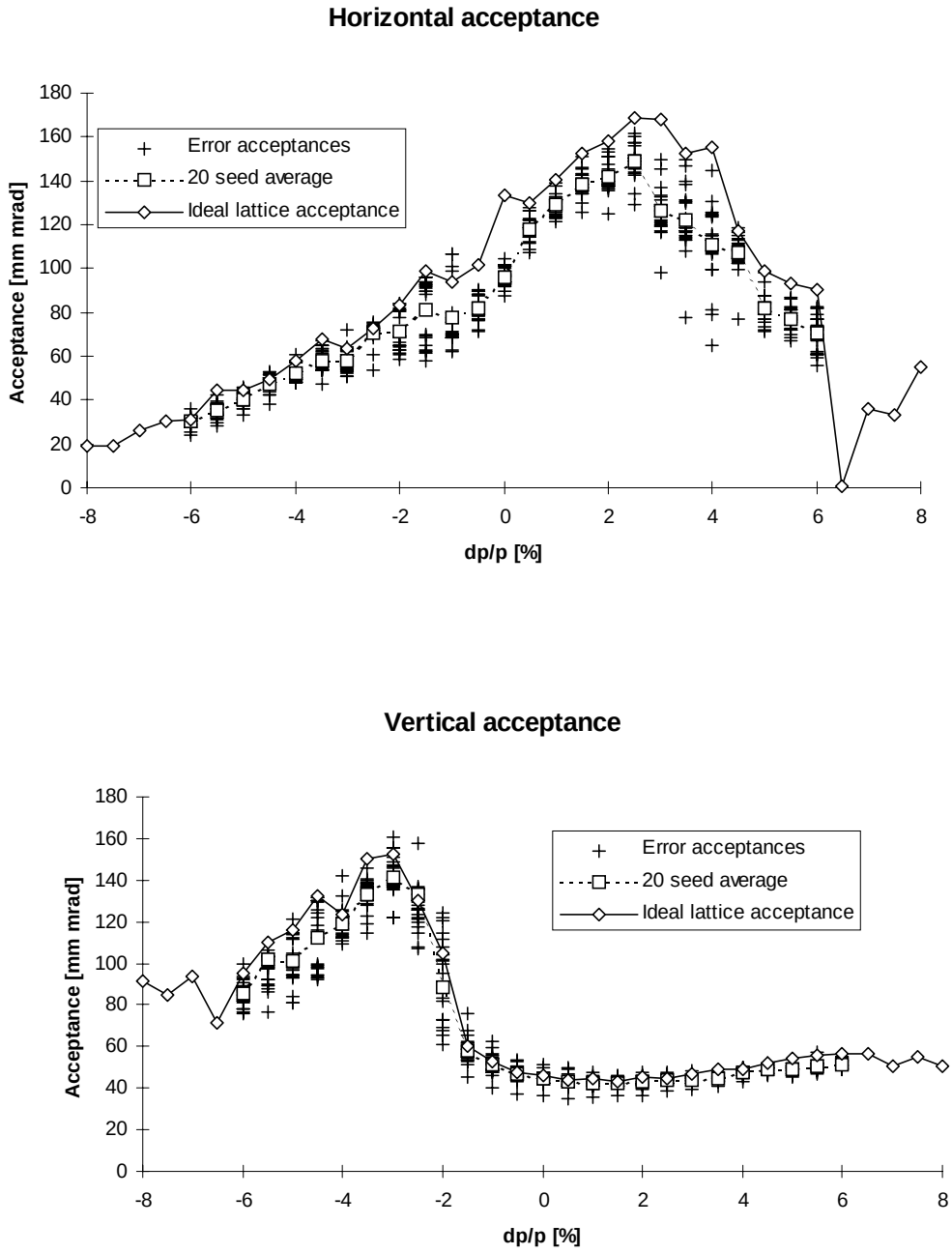

Figure f22_t: D1-mode: Horizontal and vertical dynamic acceptance as a function of relative momentum deviation for the ideal lattice and for the real lattice with displacement errors of 200 μm r.m.s. (cut at 2σ) for the girder joints, 10 μm r.m.s. (cut at 2σ) for the girder joint play and 30 μm r.m.s. (cut at 2σ) for the magnets relative to the girders (same set of 20 random seeds for every point). Displacement errors were also applied to the beam position monitors, sitting on the girders too. The closed orbit correction largely restores the acceptance values for the error free lattice. The breakdown for the horizontal ideal lattice acceptance at 6.5 % is due to the momentum dependant tune crossing an integer (see figure f22_m), and subsequent calculations with alignment errors could not find a closed orbit, therefore the acceptance scan was restricted to ±6%. (TRACY-2)